J. Neurovirol. (2015) 21:399–414
DOI 10.1007/s13365-015-0328-0

# Genetic diversity and proviral DNA load in different neural compartments of HIV-1 subtype C infection

**Mamata Mishra · Rebu K. Varghese · Anjali Verma · Sutanuka Das · Renato Santana Aguiar · Amilcar Tanuri · Anita Mahadevan · Susarla K. Shankar · Parthasarathy Satishchandra · Udaykumar Ranga**

Received: 1 August 2014 / Revised: 9 January 2015 / Accepted: 12 February 2015 / Published online: 7 March 2015


**Abstract** In India, the low prevalence of HIV-associated dementia (HAD) in the Human immunodeficiency virus type 1 (HIV-1) subtype C infection is quite paradoxical given the high-rate of macrophage infiltration into the brain. Whether the direct viral burden in individual brain compartments could be associated with the variability of the neurologic manifestations is controversial. To understand this paradox, we examined the proviral DNA load in nine different brain regions and three different peripheral tissues derived from ten human subjects at autopsy. Using a highly sensitive TaqMan probe-based real-time PCR, we determined the proviral load in multiple samples processed in parallel from each site. Unlike previously published reports, the present analysis identified uniform proviral distribution among the brain compartments examined without preferential accumulation of the DNA in any one of them. The overall viral DNA burden in the brain tissues was very low, approximately 1 viral integration per 1000 cells or less. In a subset of the tissue samples tested, the HIV DNA mostly existed in a free unintegrated form. The V3–V5 envelope sequences, demonstrated a brain-specific compartmentalization in four of the ten subjects and a phylogenetic overlap between the neural and non-neural compartments in three other subjects. The envelope sequences phylogenetically belonged to subtype C and the majority of them were R5 tropic. To the best of our knowledge, the present study represents the first analysis of the proviral burden in subtype C postmortem human brain tissues. Future studies should determine the presence of the viral antigens, the viral transcripts, and the proviral DNA, in parallel, in different brain compartments to shed more light on the significance of the viral burden on neurologic consequences of HIV infection.

**Keywords** HIV-1 · Subtype C · HIV-associated dementia · Proviral load

M. Mishra · R. K. Varghese · A. Verma · S. Das · U. Ranga (✉)
HIV-AIDS Laboratory, Molecular Biology and Genetics Unit, Jawaharlal Nehru Centre for Advanced Scientific Research, Jakkur, Bangalore, India
e-mail: udaykumar@jncasr.ac.in

R. S. Aguiar · A. Tanuri
Department of Genetics, Universidade Federal do Rio de Janeiro, Rio de Janeiro, Brazil

A. Mahadevan · S. K. Shankar
The Department of Neuropathology, National Institute of Mental Health & Neuro Sciences, Bangalore, Karnataka, India

P. Satishchandra
The Department of Neurology, National Institute of Mental Health & Neuro Sciences, Bangalore, Karnataka, India

## Introduction

Of the various subtypes of human immunodeficiency virus type I (HIV-1) and their recombinant forms, subtype C strains are responsible for approximately half of the global infections (Esparza and Bhamarapravati 2000) and nearly all the infections in India (Siddappa et al. 2005). The central nervous system (CNS) is one of the early targets of the viral infection. The monocytoid cells, including blood-derived macrophages and resident microglia, constitute the primary targets for the virus in the brain (Fischer-Smith et al. 2001). Serious neurologic complications, however, are manifested only during the later stages of the infection, coinciding with the development of AIDS (An et al. 1999; Gonzalez et al. 2000). HIV-1-associated neurocognitive disorders (HAND) may be classified into three different categories in increasing order of clinical severity-asymptomatic neurocognitive impairment (ANI), mild neurocognitive disorder (MND) and HIV-associated dementia (HAD) (Antinori et al. 2007; Zhou and Saksena 2013).

The CNS infection of subtype C differs in the clinical manifestations from that of other HIV-1 subtypes, especially in the advanced stages of the infection. In India, the incidence/prevalence of HAD among asymptomatic and drug-naive subjects is reported to be significantly low, only 1–6 % (Satishchandra et al. 2000; Wadia et al. 2001; Riedel et al. 2006; Gupta et al. 2007) as opposed to 20–35 % in the USA and Europe (Heaton et al. 1995; White et al. 1995; Sacktor et al. 2002). A few recent studies from India, employing recommended batteries of neuropsychological testing (including the International HIV dementia scale), found that ANI was manifested in a high proportion of AIDS patients, whereas MND was seen in a significantly smaller proportion and HAD was detected rarely, reconfirming the findings of the previous clinical studies. In one study, ANI was detected in 69 % of AIDS patients tested (WHO Stage III) compared to 6 % with MND and only 3 % with HAD (Muniyandi et al. 2012). Similar findings were reported in a different study of HIV-positive patients on HAART (CD4 counts >200/mm$^3$) with prevalence of 30 % of ANI, 2.5 % of MND and none with HAD (Saini and Barar 2014). In a cross-sectional survey using 132 subjects of a multiethnic South Asian population consisting of Chinese, Malay, and Indian races, the prevalence of HIV-associated dementia was reported to be as small as 1.5 % of the HAND cases while ANI and MND constituted 22.7 and 15.9 %, respectively (Chan et al. 2012). Using Luria-Nebraska scales in clinically asymptomatic HIV-positive subjects, Singh et al. identified cognitive dysfunction, but not MND or HAD in the subjects (Singh et al. 2011).

Multiple factors may underlie the low frequency of HAD in India. Unlike in the industrialized countries, the HIV epidemic in India is characterized by the presence of a huge burden of opportunistic infections of the brain which may lower the real prevalence of HAD (Shankar et al. 2005). Furthermore, the differences in the host factor landscape may also underscore the reported low prevalence of HAD in India. Interestingly, the absence of multinucleated giant cells in the brain tissues of the postmortem samples and the uniform presence of infiltrating macrophages in all the brain tissues appear to be unique for the HIV epidemic of India (Mahadevan et al. 2007). The various neurological manifestations of HIV infection, unique in the Indian context, including the rarity of HIV-associated neoplasia, the absence of a diffuse infiltrative lymphocytosis syndrome involving peripheral nerves and the rare presence of spinal cord pathology including vacuolar myelopathy even among asymptomatic cases have been reviewed (Shankar et al. 2005).

Mechanisms underlying the pathogenesis of HAD, characterized by neuronal injury and death, are many, including direct cytotoxicity of the viral proteins such as gp120, Vpr, Rev, Nef, and Tat (Zhou and Saksena 2013). The secretion of the proinflammatory cytokines and chemokines as a consequence of the viral infection is also implicated in the viral neuropathogenesis. HIV-associated dementia is directly correlated with the recruitment of activated monocytes to the brain (Glass et al. 1995; Liu et al. 2000), suggesting that the monocytes possibly trigger a cascade of events that ultimately leads to neuronal death (Persidsky et al. 2000; Gartner and Liu 2002; Gonzalez-Scarano and Martin-Garcia 2005). A dicysteine motif in Tat has been implicated in direct monocyte chemotaxis in vitro (Albini et al. 1998). Importantly, we previously demonstrated that of all the HIV-1 genetic subtypes, in subtype C Tat alone, the dicysteine motif (C30C31) essential for the chemotactic function exhibits a C31S polymorphism making it a compromised monocyte chemokine (Ranga et al. 2004). Reconstitution of the dicysteine motif in subtype C Tat made the viral protein as toxic as the subtype B counterpart to primary neurons in a severe combined immune deficiency (SCID) mouse HIV encephalitis model (Rao et al. 2008).

The low prevalence of HIV-associated dementia in India is quite paradoxical, especially in the light of the heavy macrophage infiltration demonstrated in all the brain compartments examined (Mahadevan et al. 2007). The severity of dementia was shown to be correlated with the magnitude of the macrophage infiltration to the brain (Glass et al. 1993). In an attempt to explain the differences in the severity of neuropathological manifestation in HIV infection, Wiley et al. proposed a possible association between the local viral burden in the brain compartments and neurologic complications (Wiley et al. 1994). Using a range of techniques, including PCR for the amplification of the viral nucleic acids and/or immunohistochemistry for viral antigens, the relative abundance of the viral infection of various brain tissues was quantitated by many groups. A direct correlation between the RNA viral load in the brain or the levels of the viral antigens and the severity of neurological manifestations was demonstrated in the SIV pigtailed macaque experimental model (Zink et al. 1999). In the human infection, however, a correlation of this nature was either weak (An et al. 1996; Lazarini et al. 1997; Fujimura et al. 1997) or absent (Glass et al. 1995; Johnson et al. 1996). Given the rare occurrence of dementia in the subtype C infection of India, it was not practically feasible to design a study to compare the association between the severity of the neurological manifestations and the burden of the viral infection in the brain tissues. We instead attempted to ask if the proviral load in the brain tissues would differ in different compartments of the brain in the Indian scenario. We demonstrate that the proviral burden in various brain compartments was broadly uniform without a preferential accumulation of the viral DNA in any specific compartment.

## Results

### Phylogenetic analysis of the envelope sequences

Tissue samples from different neural and peripheral tissues collected at autopsy were available from 10 HIV-1

seropositive diseased subjects, for the present study (Table 1). All the subjects were adults and with the exception of one individual (A26-10), all were drug-naive. The CD4 cell count and the viral load details were not available for many of the subjects due to short hospital stay prior to death. Importantly, a majority of the study subjects, 7 of 10, contained one or the other opportunistic infection of the brain as summarized in the table. Three of the 10 subjects (cases 4, 7, and 10) do not have an OI. Cases 4 and 7 have Guillain–Barre (GB) syndrome (an immune mediated neuropathy) and case 7 died of a road traffic accident.

A 703-bp gene segment of the envelope spanning V3–V5 was amplified from the genomic DNA extracted from different brain compartments available for each subject using the nested-PCR strategy. The brain compartments consisted of the frontal cortex, hippocampus, caudate nucleus putamen, thalamus, amygdala, cerebellum, cervical cord and choroid plexus. Additionally, the envelope segment was also amplified from a few peripheral compartments consisting of the liver, lymph node (paratracheal), and spleen. We isolated multiple samples from each compartment and processed them simultaneously as well as repeated the extraction procedure to enhance the chances of successful amplification. We could successfully amplify the envelope gene segment from nine of the ten subjects from different neural and peripheral compartments. From subject A26-10, who was on antiretroviral therapy, however, we could amplify the envelope sequence only from two peripheral tissues, the paratracheal lymph node and the spleen.

The envelope sequences were aligned, manually edited, gap-stripped and a neighbor-joining tree was constructed to infer the phylogenetic relationship (Fig. 1). All the envelope sequences clustered with the two subtype C reference sequences and separated clearly from the non-subtype C reference sequences (A, B, D, F1, G, and H) ascertaining that all the infecting viral strains in our cases phylogenetically belonged to subtype C. The sequences also clustered in a subject-specific manner. Interestingly, in subject MLC221-05, the sequences derived from two brain compartments (frontal cortex and hippocampus) clustered separately from sequences derived from three other compartments (cerebellum, thalamus, and lymph node) from the same individual. Incidentally, only these two sequences were found to be X4- or dual-tropic in a subsequent analysis (see below). In three subjects (A1-13, A46-06, and M03-11) env sequences only from the neural compartments were available. In a subset of four subjects (A15-11, MLC221-05, A46-06, and A26-10), a phylogenetic separation was evident between the neural and non-neural tissues. In the rest of the three subjects (A32-11, A20-12, and M316-11), phylogenetic separation between the neural and non-neural tissues was not seen as the sequences from these two compartments mixed freely implying free migration of viral strains between different tissue compartments.

**Table 1** The clinical profile of the study subjects

| Case | Autopsy ID | Age/sex | PMI (hrs) | ART | CD4 counts/mm$^3$ | Diagnosis |
|---|---|---|---|---|---|---|
| 1 | MLC221-05 | 45/M | 19.5 | Naïve | ND | DTB |
| 2 | A44-06 | 38/F | 4.0 | Naïve | ND | CM |
| 3 | A46-06 | 36/F | 4.2 | Naïve | ND | TE |
| 4 | A26-10 | 40/F | 7.2 | ART | 586 | GBS |
| 5 | M03-11 | 50/M | NA | Naïve | ND | TE |
| 6 | A15-11 | 55/F | NA | Naïve | 30 | DTB |
| 7 | M316-11 | 25/F | 7.3 | Naïve | 30 | RTA |
| 8 | A32-11 | 35/F | 2.3 | Naïve | 11 | CM |
| 9 | A20-12 | 45/F | NA | Naïve | ND | TE |
| 10 | A01-13 | 35/F | NA | Naïve | ND | GBS |

*ART* antiretroviral therapy, *CM* crytococcal meningitis, *DTB* disseminated tuberculosis, *GBS* Guillain–Barre syndrome, *F* female, *hrs* hours, *ID* identification number, *M* male, *NA* not available, *ND* not done, *PMI* postmortem interval, *RTA* road traffic accident, *TE* toxoplasma encephalitis

## Genetic analysis of the V3 loop

The V3 loop of HIV-1 envelope plays a critical role in determining the cellular tropism of the viral strain and importantly the coreceptor preference (Hartley et al. 2005). Additionally, a switch from CCR5 to CXCR4 use is also suggestive of the disease progression. Given the prognostic value of the coreceptor switch for disease progression, several algorithms have been developed to predict the coreceptor preference of the V3 loop. We examined several molecular properties of the env sequences and applied the algorithms to predict the coreceptor requirement of the V3 sequences. The multiple sequence alignment of the amino acid residues of the V3 loop demonstrated that the V3 loop was largely conserved across the viral strains (Fig. 2). Many molecular features within V3, characteristic of subtype C and suggestive of CCR5 preference were preserved. The V3 loop in all the viral strains comprised of 35 amino acid residues with the exception of subject MLC221-05 where the loop contained only 34 residues. The crown of V3 loop in the majority of the viral strains contained the GPGQ motif, which is characteristic of subtype C, unlike in other viral subtypes that usually contain the GPGR motif. The GPGQ motif, highly suggestive of CCR5 use (Cilliers et al. 2003), was seen among the viral strains derived from all the 10 subjects regardless of the tissue differences. Of note, in subject MLC221-05, sequences derived from two different neural compartments (frontal cortex and hippocampus) appeared exceptional in containing a GPGK motif. Interestingly, these two sequences were predicted to be dual-tropic or X4-tropic viruses by two different algorithms (Table 2).

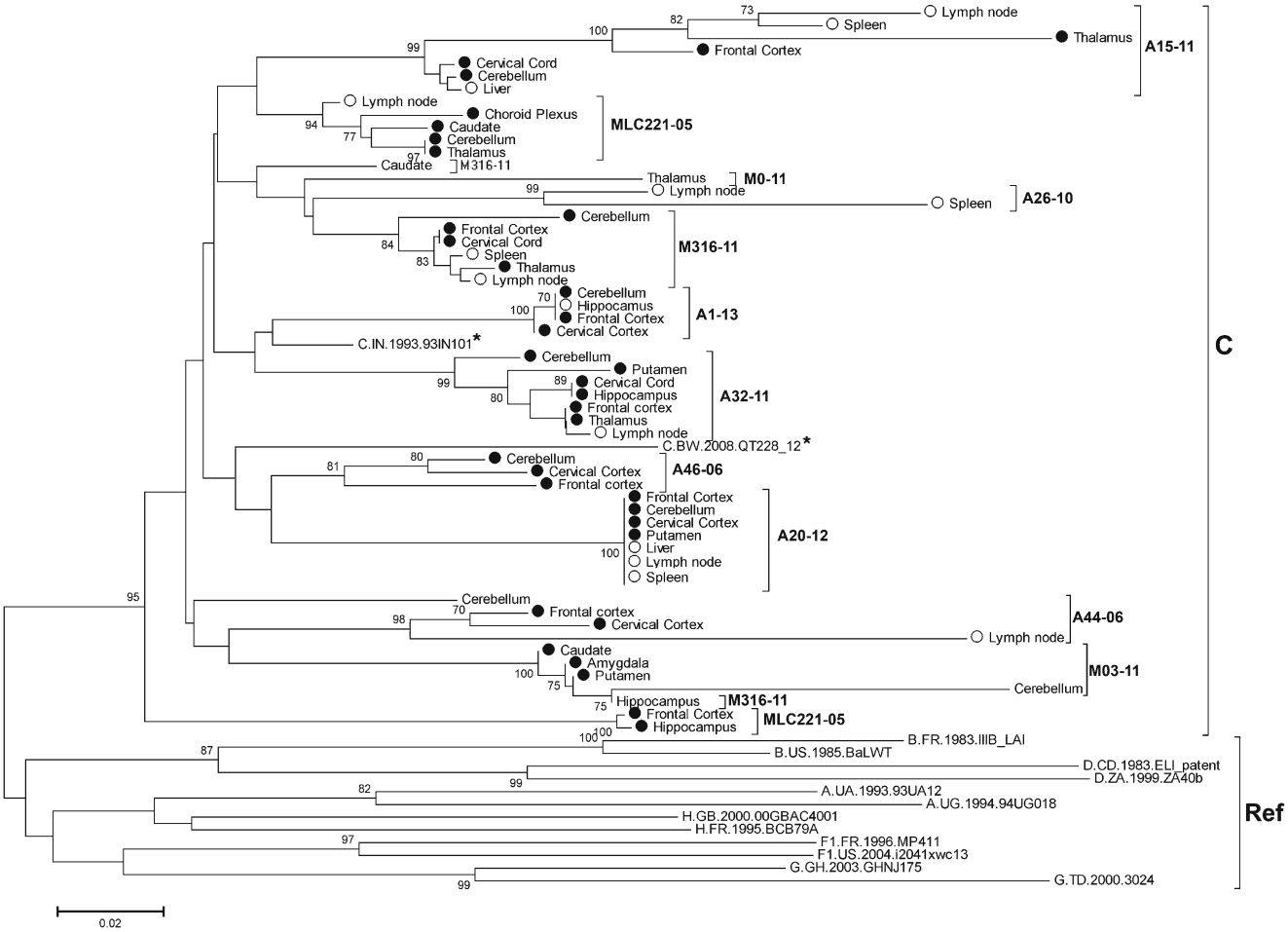


**Fig. 1** Phylogenetic analysis of the envelope sequences: Neighbor-joining phylogenetic tree of 54 HIV-1 envelope (V3–V5) sequences (249 bp) derived from nine different neural and three non-neural tissue samples of ten subjects at post-mortem. *Filled and open circles* represent the sequences of neural and non-neural origin, respectively. The reference sequences representing the viral subtypes were downloaded from the HIV sequence database. The two subtype C reference sequences are identified with an *asterisk*. Horizontal branch lengths are to the scale of 0.02 nucleotide substitution per site. Vertical separation is only for clarity. Values at the nodes indicate the percentage bootstrap values that support branching out of a total of 1000 resamplings. The bootstrap values 70 % and higher are shown. *C* subtype C, *Ref* reference sequences

The presence of the basic amino acids arginine and lysine at positions 306 and 322 is characteristic of subtype B and in subtype C these residues are replaced by serine and isoleucine, respectively (Zhang et al. 2010). Serine 306 and isoleucine 322 were highly conserved in nearly all the viral sequences (Fig. 2).

The presence of a neutral serine at position 11 and of an aspartic acid or aspargine with a negatively charged side chain at position 25 is suggestive of CCR5 use (Jensen et al. 2006). While nearly all the V3 sequences in our samples contained a serine residue at position11, a large majority of the viruses contained an aspartic acid or an asparigine residue at position 25 (Table 2). Interestingly, the two MLC221-05 sequences derived from the frontal cortex and hippocampus demonstrated a deletion of the aspartic acid at position 25 although they retained serine at position 11. Furthermore, the net charge of the V3 loop is also suggestive of the coreceptor use of the envelope (Briggs et al. 2000). A net charge of 4 or a lower value is indicative of CCR5 use and a charge 5 or above is suggestive of dual- or X4-tropism. With the exception of the two MLC221-05 sequences derived from the frontal cortex and hippocampus, all the other V3 sequences contained a net charge of 4 or less (Table 2) suggesting that the envelopes may preferably use CCR5 for infection. Furthermore, the V3 loop typically contains a single N-glycosylation site (NNTR), the preservation of which is suggestive of CCR5 use and the loss of CXCR4 use (Pollakis et al. 2001). All the V3 sequences with the exception of one (frontal cortex of A46-06) preserved the N-glycosylation site.

The position-specific scoring matrix (PSSM) strategy demonstrated not only improved predictive power for subtype C (Jensen et al. 2003), but also proved to be more efficient in analyzing the transition from CCR5 to CXCR4 use in subtype B. With the exception of a small number of

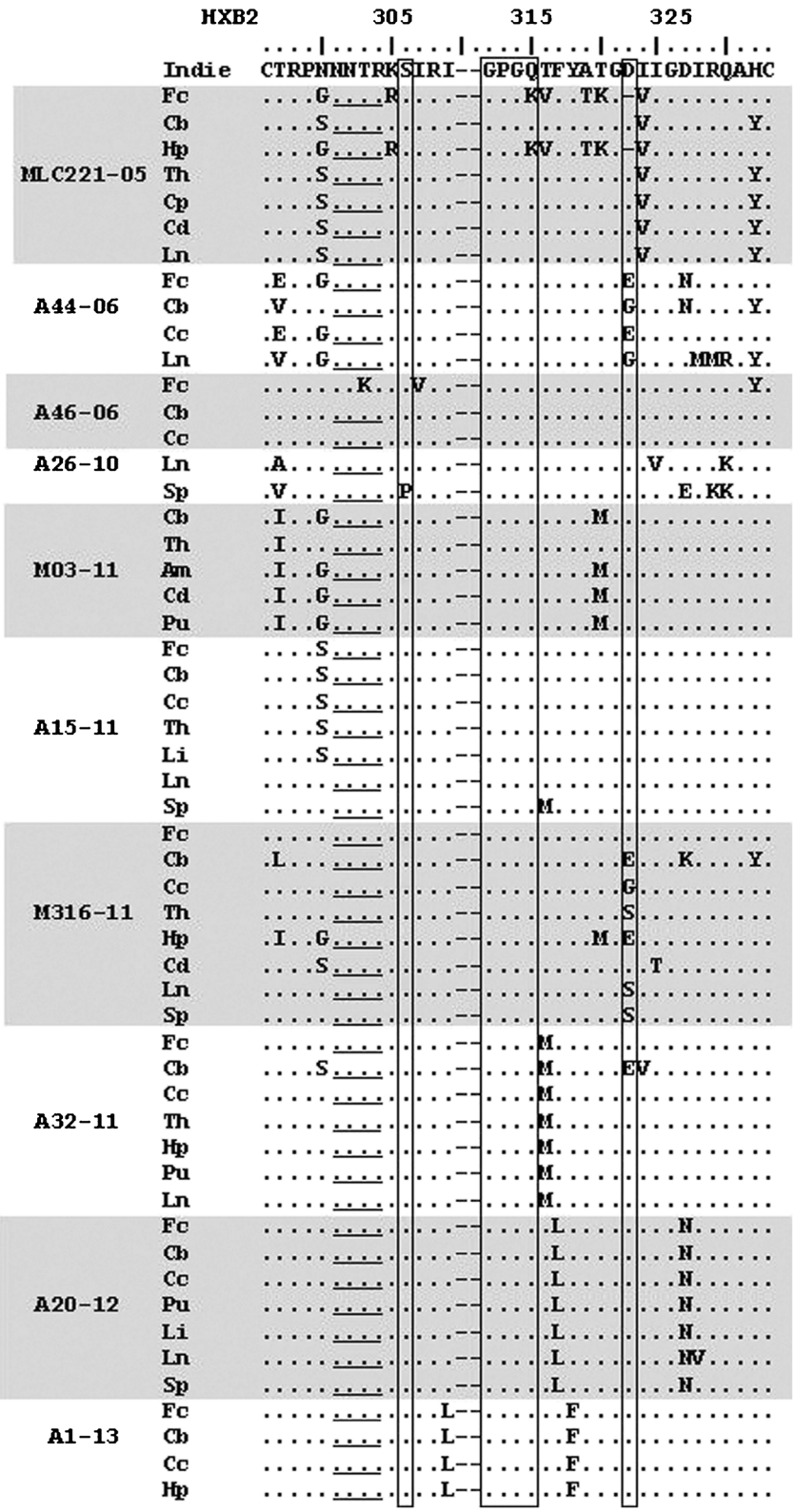


**Fig. 2** Multiple sequence alignment of the V3-loop amino acid residues: The 35 amino acid residues constituting the V3-loop of HIV-1 env and derived from different neural and non-neural tissues of 10 subjects are aligned with subtype C reference molecular clone Indie-C1 sequence (AB023804) at the top. The sequence coordinates, however, are as per HXB2. The patient and tissue identity numbers are shown on the left side. *Dots* indicate sequence homology and the *dashes*, gaps. The "GPGQ" motif and the positions 11 and 25 are highlighted using *square boxes*. The potential N-linked glycosylation site is *underlined*. *Am* amygdala, *Cb* cerebellum, *Cc* cervical cord, *Cd* caudate, *Cp* choroid plexus, *Fc* frontal cortex, *Hp* hippocampus, *Ln* lymph node, *Li* LIVER, *Pu* putamen, *Sp* spleen, *Th* thalamus

viral strains (frontal and hippocampus of MLC221-05, lymph node of A44-06, spleen of A26-10), the large majority of the V3 sequences were found to be R5-tropic (Table 2). The application of the geno2pheno predictor too provided comparable results. Collectively, the above results suggested that the large majority of the viral V3 loop sequences derived from diverse neural and peripheral tissues demonstrated a preference for CCR5.

**Table 2** Genetic analysis of the envelope (V3–V5)

| Tissue ID | | PNGS | | | | PSSM score | | FPR% | V3[a] | Aa 11,25 |
|---|---|---|---|---|---|---|---|---|---|---|
| | | V3 | V4 | V5 | V3–V5 | *C* | *B* | | | |
| | HXB2 | 36,1 | 34,4 | 13,1 | 177,10 | −2.90, X4 | 3.47, X4 | 0,X4 | 9,9 | RK |
| | Indie | 35,1 | 32,4 | 17,2 | 177,12 | −29.93, R5 | −9.06, R5 | 83,R5 | 6,4 | SD |
| MLC221-05 | Fc | 34,1 | 21,3 | 16,1 | 160,11 | −11.88, R5X4 or X4 | 8.603, R5X4 or X4 | 1.7, X4 | 8,7 | S- |
| | Cb | 35,1 | 29,2 | 17,0 | 174,8 | −28.21, R5 | −8.131, R5 | 76.5, R5 | 5,3 | SD |
| | Hp | 34,1 | 21,3 | 16,1 | 160,11 | −11.88, R5X4 or X4 | 8.603, R5X4 or X4 | 1.7, X4 | 8,7 | S- |
| | Th | 35,1 | 29,4 | 17,1 | 174,11 | −28.21, R5 | −8.131, R5 | 76.5, R5 | 5,3 | SD |
| | Cp | 35,1 | 28,0 | 17,0 | 173,8 | −28.21, R5 | −8.131, R5 | 76.5, R5 | 5,3 | SD |
| | Cd | 35,1 | 29,4 | 17,1 | 173,11 | −28.21, R5 | −8.407, R5 | 76.5, R5 | 5,3 | SD |
| | Ln | 35,1 | 29,4 | 16,1 | 172,10 | −28.21, R5 | −8.131, R5 | 76.5, R5 | 5,3 | SD |
| A44-06 | Fc | 35,1 | 31,3 | 10,1 | 167,11 | −25.17, R5 | −8.407, R5 | 71.2, R5 | 6,4 | SE |
| | Cb | 35,1 | 30,3 | X | 173,2 | −27.92, R5 | −6.339, R5 | 74.4, R5 | 5,4 | SG |
| | Cc | 35,1 | 30,3 | 15,0 | 173,3 | −25.62, R5 | −9.234, R5 | 64.0, R5 | 6,3 | SE |
| | Ln | 35,1 | 30,1 | 24,0 | 183,2 | −19.80, R5 | −1.240, R5X4 or X4 | 19.5, R5 | 5,4 | SG |
| A46-06 | Fc | 35,1 | 29,6 | 17,1 | 172,12 | −25.59, R5 | −4.122, R5 | 17.1, R5 | 6,4 | SD |
| | Cb | 35,1 | 25,4 | 18,0 | 173,8 | −29.93, R5 | −9.057, R5 | 83.0, R5 | 6,4 | SD |
| | Cc | 35,1 | 25,5 | X | 114,8 $ | −25.62, R5 | −9.234, R5 | 83.0, R5 | 6,3 | SD |
| A26-10 | Ln | 35,1 | 35,4 | 17,2 | 178,12 | −24.7, R5 | −5.551, R5 | 30.1, R5 | 7,5 | SD |
| | Sp | 35,1 | 34,0 | 15,0 | 179,4 | −21.9, R5 | −0.558, R5X4 or X4 | 74.3, R5 | 7,5 | PD |
| M03-11 | Cb | 35,1 | 31,4 | 12,0 | 172,13 | −25.36, R5 | −8.86, R5 | 51.6,R5 | 6,4 | SD |
| | Th | 35,1 | 27,5 | 16,1 | 169,13 | −28.44, R5 | −9.126, R5 | 76.7, R5 | 6,4 | SD |
| | Am | 35,1 | 32,4 | 14,1 | 172,13 | −25.36, R5 | −8.863, R5 | 51.6, R5 | 6,4 | SD |
| | Cd | 35,1 | 32,4 | 14,1 | 172,13 | −25.36, R5 | −8.863, R5 | 51.6, R5 | 6,4 | SD |
| | Pu | 35,1 | 32,4 | 14,1 | 172,13 | −25.36, R5 | −8.863, R5 | 51.6, R5 | 6,4 | SD |
| A15-11 | Fc | 35,1 | 24,4 | 14,0 | 162,8 | −30.5, R5 | −9.565, R5 | 86.9, R5 | 6,4 | SD |
| | Cb | 35,1 | 24,3 | 15,1 | 163,11 | −30.5, R5 | −9.565, R5 | 86.9, R5 | 6,4 | SD |
| | Cc | 35,1 | 24,3 | 15,1 | 163,11 | −30.5, R5 | −9.565, R5 | 86.9, R5 | 6,4 | SD |
| | Th | 35,1 | 23,0 | 14,0 | 163,3 | −30.5, R5 | −9.565, R5 | 86.9, R5 | 6,4 | SD |
| | Ln | 35,1 | 24,3 | 13,0 | 173,6 | −29.93, R5 | −9.057, R5 | 83.0, R5 | 6,4 | SD |
| | Sp | 35,1 | 25,2 | 14,0 | 173,4 | −29.93, R5 | −9.057, R5 | 83.0, R5 | 6,4 | SD |
| M316-11 | Fc | 35,1 | 34,4 | 15,2 | 170,12 | −29.93, R5 | −9.057, R5 | 83.0, R5 | 6,4 | SD |
| | Cb | 35,1 | 30,4 | 14,2 | 170,12 | −24.45, R5 | −5.613, R5 | 59.0, R5 | 6,5 | SE |
| | Cc | 35,1 | 30,4 | 15,2 | 170,12 | −28.06, R5 | −7.636, R5 | 66.0, R5 | 6,5 | SG |
| | Th | 35,1 | 30,4 | 15,2 | 170,11 | −27.0, R5 | −6.473, R5 | 82.9, R5 | 6,5 | SS |
| | Cd | 35,1 | 30,5 | 17,2 | 173,13 | −27.49, R5 | −8.86, R5 | 89.3,R5 | 6,4 | SE |
| | Hp | 35,1 | 31,5 | 14,1 | 172,13 | −24.48, R5 | −9.169, R5 | 42.3, R5 | 6,4 | SD |
| | Ln | 35,1 | 30,4 | 17,2 | 170,13 | −27.0, R5 | −6.473, R5 | 82.6, R5 | 6,5 | SS |
| | Sp | 35,1 | 30,4 | 15,2 | 170,12 | −27.0, R5 | −6.473, R5 | 69.5, R5 | 6,5 | SS |
| A32-11 | Fc | 35,1 | 31,5 | 16,0 | 174,12 | −26.92, R5 | −8.834, R5 | 52.1, R5 | 6,4 | SD |
| | Cb | 35,1 | 31,5 | 17,1 | 175,13 | −24.64, R5 | −9.146, R5 | 69.5, R5 | 6,4 | SE |
| | Cc | 35,1 | 31,5 | 16,1 | 174,13 | −26.92, R5 | −8.834, R5 | 69.5, R5 | 6,4 | SD |
| | Th | 35,1 | 31,5 | 16,1 | 174,13 | −26.92, R5 | −8.834, R5 | 69.5, R5 | 6,4 | SD |
| | Hp | 35,1 | 31,5 | 16,1 | 174,11 | −26.92, R5 | −8.834, R5 | 86.9, R5 | 6,4 | SD |
| | Pu | 35,1 | 31,5 | 16,1 | 174,13 | −26.92, R5 | −8.834, R5 | 69.5, R5 | 6,5 | SD |
| | Ln | 35,1 | 31,4 | 16,0 | 174,11 | −26.92, R5 | −8.834, R5 | 96.0, R5 | 6,4 | SD |
| A20-12 | Fc | 35,1 | 26,5 | 15,1 | 165,11 | −26.28, R5 | −7.291, R5 | 96.0, R5 | 6,5 | SD |
| | Cb | 35,1 | 25,1 | 13,0 | 175,5 | −26.28, R5 | −7.291, R5 | 96.0, R5 | 6,5 | SD |
| | Cc | 35,1 | 26,5 | 15,1 | 165,11 | −26.28, R5 | −7.291, R5 | 96.0, R5 | 6,5 | SD |

**Table 2** (continued)

| Tissue ID | | PNGS | | | | PSSM score | | FPR% | V3[a] | Aa 11,25 |
|---|---|---|---|---|---|---|---|---|---|---|
| | | V3 | V4 | V5 | V3–V5 | *C* | *B* | | | |
| | Pu | 35,1 | 26,5 | 15,1 | 165,11 | −26.28, R5 | −7.291, R5 | 96.0, R5 | 6,5 | SD |
| | Li | 35,1 | 26,5 | 15,1 | 165,11 | −26.28, R5 | −7.291, R5 | 96.0, R5 | 6,5 | SD |
| | Ln | 35,1 | 26,5 | 15,1 | 165,11 | −26.28, R5 | −6.629, R5 | 89.1, R5 | 6,5 | SD |
| | Sp | 35,1 | 26,5 | 15,1 | 165,11 | −26.28, R5 | −7.291, R5 | 86.9, R5 | 6,5 | SD |
| A01-13 | Fc | 35,1 | 28,4 | 17,2 | 171,12 | −25.81, R5 | −9.436, R5 | 89.6, R5 | 6,4 | SD |
| | Cb | 35,1 | 28,4 | 17,2 | 171,12 | −25.81, R5 | −9.436, R5 | 89.6, R5 | 6,4 | SD |
| | Cc | 35,1 | 28,4 | 17,2 | 171,12 | −25.81, R5 | −9.436, R5 | 89.6, R5 | 6,4 | SD |
| | Hp | 35,1 | 28,4 | 17,2 | 171,12 | −25.81, R5 | −9.436, R5 | 89.6, R5 | 6,4 | SD |

*PNGS* potential *N*-glycosylation sites, *PSSM* position-specific scored matrix, *FPR* false positive rate, *X* not available, *$* only V3–V4

[a] Net charge, positive charge

## Genetic analysis of the non-V3 loop sequences

Non-V3 env loops (V1/V2, V4, and V5) are known to influence several biological properties of the envelope including the coreceptor switching (Hartley et al. 2005). To examine the molecular features suggestive of such biological influences, we aligned amino acid sequences spanning C3, V4, C4, and V5 derived from the clinical samples (Fig. 3). While both the constant domains C3 and C4 were relatively conserved, the variable regions V4 and V5 were highly variable among the subjects. Especially the length of the V4 loop was significantly shorter due to extensive deletion of the amino acid residues in all the study subjects. While the V4 loop consisted of 32 amino acid residues in Indie-C1, the reference subtype C molecular clone, the number of the residues was shorter in the V4 loop comprising of as few as 21 residues in most of the subjects and in many of the tissues. The number of PNGS varied broadly spanning from no PNGS (choroid plexus of subject MLC221-05) to having as many as 7 (frontal cortex of subject A15/1). The V5 loop, unlike V4, did not vary much with respect to amino acid length and the number of PNGS.

## Quantification of proviral DNA copy number in the neural compartments

In addition to the nature of the viral antigens, the viral burden may directly contribute to neuropathogenesis in HIV infection of the brain (An et al. 1996). It is not understood if the viral load in different brain compartments could be varied in an infected subject and at different stages of the viral infection and how such a variation might impact the pathological manifestations (Bell et al. 1993). To address some of these questions, we developed a highly sensitive TaqMan probe-based real-time PCR, using the primer pair N2185 and N2186 and targeting a highly conserved region within the U5-PBS region, with a detection sensitivity of less than 10 copies of the integrated virus. Proviral load of HIV-1 was determined in the 10 subjects from the available samples of 9 different brain compartments and three different peripheral tissues (Table 3). Unfortunately, in some subjects, the availability of the tissues was restricted to a few compartments. The analysis led to three or four important observations.

First, the proviral load in the brain tissues was found to be low to moderate often ranging in single to three digits per microgram of genomic DNA or 0.14 million brain cells. Regardless of the low copy number, the presence of the viral DNA could be detected and quantitated in all the brain compartments in 5 of the 10 subjects (A44-06, A46-06, A15-11, A32-11, and A01-13). In subject A32-11, for instance, samples from seven different brain compartments were available and the presence of the viral DNA was detected in all the seven compartments. In two other subjects (M03-11 and A20-12), the viral DNA was identified in five of the six brain compartments. The other three subjects belonged to the low copy group. In subjects MLC221-05 and M316-11, the virus was found only in 2/6 and 1/6 brain compartments, respectively. In these two subjects, only a single sample out of five or ten independent samples, within a compartment demonstrated amplification suggesting extremely low viral burden. In subject A26-10, the only person on antiretroviral therapy, the virus could not be amplified from any of the nine brain compartments and two of the three peripheral compartments. In this subject, only in the spleen, only one of the five samples demonstrated amplification at very low copy number.

Second, the data collectively suggested a uniform distribution of the viral infection across the different compartments of the brain especially when five of the nine brain tissues (frontal cortex, cerebellum, putamen, thalamus, and cervical cord), for which a large number of samples were available, were compared (Table 3). Unlike a few of the previous reports, we did not find uneven accumulation of the viral DNA in any single brain compartment. For instance, the mean viral load values in

the frontal cortex ($n$=35 derived from eight subjects), cerebellum ($n$=35 derived from seven subjects) and cervical spinal cord ($n$=28 derived from six subjects) 94.9±339.5, 101.5±314.5, and 91.1±247.2, respectively, were not significantly different from one another. Third, a comparison of the viral DNA load between the neural and peripheral compartments demonstrated a significant difference. The presence of the virus was readily detected in the spleen and the paratracheal lymph node, but not in the liver. Although the non-availability of samples in many subjects hampered a meaningful interpretation, the mean viral load levels were significantly higher in the two peripheral tissues (the lymph node and the spleen) as compared to three neural tissues (frontal cortex, cerebellum, and cervical cord). While the mean viral loads in the lymph node and the spleen were 449.4±787.9 ($n$=22 derived from five subjects) and 210.5±318.0 ($n$=21 derived from four subjects), respectively. The combined mean viral load of these two peripheral compartments 332.7±610.9 ($n$=43 derived from six subjects) was significantly higher ($p$=0.001) than that of all of the three neural compartments (the frontal cortex, cerebellum, and cervical cord) 96.2±303.5 ($n$=98 derived from ten subjects). The mean viral load in the peripheral compartment, thus, appears to be three- to four-fold higher as compared to that of the neural compartment. Lastly, using a nested Alu-PCR strategy, we found that a large proportion of the viral DNA in the brain tissues remained in unintegrated form and that the ratio between the integrated and unintegrated viral DNA is variable from tissue to tissue. For this analysis, we randomly selected four different subjects (A44-06, M03-11, A15-11, and A32-11) and seven different tissues to examine what proportion of the viral DNA in the tissues exists in the integrated form. We performed the real-time PCR, as described above, using the primer pair N2185 and N2186, to determine the total number of the viral DNA copy numbers in the brain tissues. This real-time PCR detects both the integrated and unintegrated viral DNA forms regardless of the integration status. Additionally, we performed a nested Alu-PCR to determine the number of proviral copies that exist only in

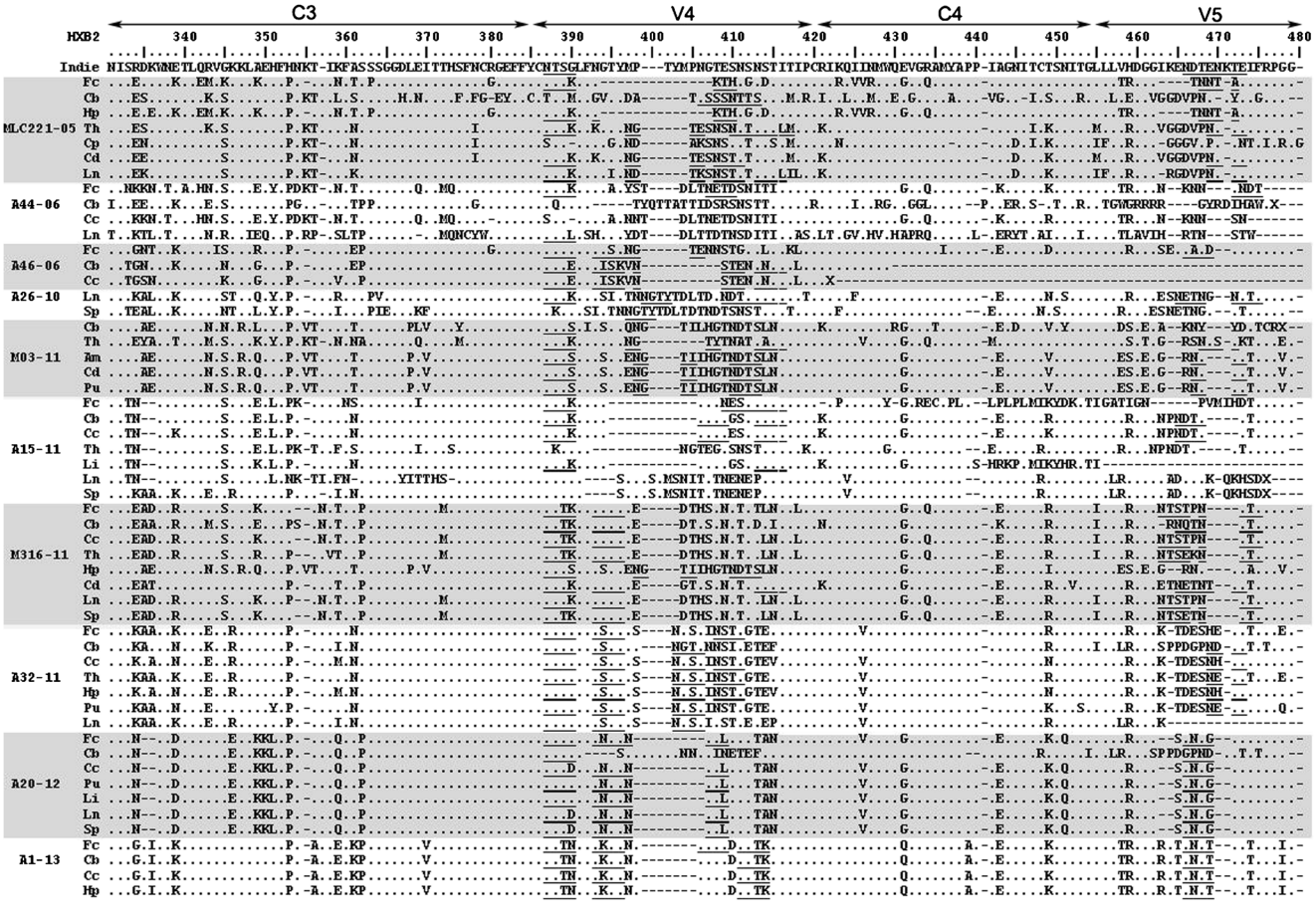


**Fig. 3** Multiple amino acid sequence alignment of C3, V4, C4, and V5 regions: The amino acid residues spanning C3-V5 and derived from different neural and non-neural tissues of 10 subjects are aligned with subtype C reference molecular clone Indie-C1 sequence (AB023804) at the top. The sequence coordinates, however, are as per HXB2. The patient and tissue identity *numbers* are shown on the left side. *Dots* indicate sequence homology and the dashes gaps. The potential N-linked glycosylation sites are *underlined. Am* amygdala, *Cb* cerebellum, *Cc* cervical cord, *Cd* caudate, *Cp* choroid plexus, *Fc* frontal cortex, *Hp* hippocampus, *Ln* lymph node, *Li* liver, *Pu* putamen, *Sp* spleen, *Th* thalamus

**Table 3** Proviral DNA load in different neural and non-neural tissues

| | Proviral copies/μg of genomic DNA (±SD) | | | | | | | | | | | |
|---|---|---|---|---|---|---|---|---|---|---|---|---|
| | Neural | | | | | | | | | Non-neural | | |
| Tissue ID | Fc | Cb | Cc | Th | Pu | Hp | Cd | Am | Cp | Ln | Sp | Li |
| MLC221-05 | 7.8 | 4.4 | X | ND | X | ND | ND | X | ND | ND | X | X |
| A44-06 | 23.4(±14.2) | 324.3(±584.0) | 364.4(±629.0) | X | X | X | X | X | X | 1203(±1197.0) | 451.3(±111.8) | 112.2(±52.9) |
| A46-06 | 7.4(±1.18) | 16.5(±6.8) | 63.7(±112.0) | X | X | X | X | X | X | X | X | X |
| A26-10 | ND | ND | ND | X | X | X | X | X | X | ND | 3.0 | X |
| M03-11 | 5.6(±4.0) | 6.6(±7.1) | X | 818.8(±1110.0) | 56.2(±58.4) | X | 33.0(±23.4) | ND | X | X | 10.6(±2.9) | ND |
| A15-11 | 70.4(±138.0) | 15.7(±15.1) | 27.2(±25.0) | 8.9(±4.7) | X | X | X | X | X | 371.6(±443.0) | 274.0(±494.0) | ND |
| M316-11 | 60.3 | ND | ND | ND | X | ND | ND | X | X | 7.4 | ND | X |
| A32-11 | 598(±949.0) | 22.6(±25.6) | 28.6(±9.8) | 65.1(±56.0) | 1771.0(±1784.0) | 186.0(±170.0) | X | 268.4(±448.3) | X | 58.2(±26.5) | X | X |
| A20-12 | 23.2(±19.4) | ND | 14.9(±12.6) | 21.0(±313.0) | 319.3 | X | X | X | X | 104.0(±54.0) | 6.0(±3.2) | ND |
| A01-13 | 59.7(±29.0) | 68.8(±73.2) | 136.0(±42.3) | X | X | 97.2(±80.0) | X | X | X | X | X | X |
| Average Stdev | 94.9(±339.5) | 101.5(±314.5) | 91.0(±247.2) | | | | | | | 449.4(±787.9) | 210.5(±318.0) | |

*Am* amygdala, *Bg* basal ganglia, *Cb* cerebellum, *Cc* cervical cord, *Cd* caudate, *Cp* chord plexus, *Fc* frontal cortex, *Hp* hippocampus, *Li* liver, *Ln* lymph node, *ND* not detectable, *Pu* putamen, *Sp* spleen, *Th* thalamus, *X* sample not available

the integrated form as described previously with a few modifications (Bachu et al. 2012). The first round of the PCR amplifies a population of the diverse integration events as the forward primer targets a highly conserved region in the R region of the 3′ LTR and the reverse primer anneals to a conserved sequence in the highly repetitive *Alu* sequence in the human genome. The second round of the PCR, using an inner set of primers, amplifies a 103-bp fragment spanning the R-U5 region within the 3′ LTR. Using a Jurkat cell population containing a reporter virus stably integrated in diverse locations of the genomic DNA, we generated a standard curve and determined the absolute copy number of the integrated proviral copies from each of the selected samples using the regression analysis. Thus, using these two different amplification strategies, we simultaneously determined the total and integrated viral DNA copies in the seven clinical samples selected randomly (Fig. 4). The difference between the two numbers is considered as the copy number of the unintegrated DNA. The analysis showed that in most of the clinical samples tested, the proportion of the unintegrated viral DNA was significantly larger than the integrated DNA. The ratio between the integrated and unintegrated DNA varied broadly across the samples. The proportion of the unintegrated viral DNA varied from as high as 86.7 % (Cc of A44-06) to as low as 67.0 % (Th of M03-11). In five of the seven clinical samples (Cb, Cc, and Ln of A44-06, Ln of A15-11 and Pu of A32-11), more than 80 % of the detected viral DNA existed in the unintegrated form. In the cerebellum of subject A44-06 for instance, we found 1550.1±1808.9 and 237.8±273.6 copies of the viral DNA per microgram of genomic DNA, in the unintegrated and integrated forms, respectively. These values were 187.2 ±152.8 and 92.2±81.5 copies, respectively, for the unintegrated and integrated forms of DNA in thalamus of subject M03-11. In other words, for every copy of integrated viral DNA, 2 to 6.5 copies of the viral DNA were found in the unintegrated form in the brain tissues tested. Our data are consistent with the previous reports that in the brain tissues a larger proportion of the viral DNA exists in an unintegrated form (Shaw et al. 1985; Pang et al. 1990; Teo et al. 1997).

## Discussion

The primary aim of the present study is to examine the pattern of the proviral load distribution in different compartments of the human brain in subtype C infection. To this end, we used a highly sensitive real-time PCR to determine the absolute numbers of the proviral DNA in the genomic DNA of the brain tissues of ten different subjects. Although the proviral DNA viral load is not representative of the active viral replication, a significant association was reported between the viral RNA load and the proviral DNA load previously (Novitsky et al. 2009). Importantly, the proviral load can represent a more sensitive assay since both integrated and unintegrated forms of the viral DNA can be detected. Our own data (Fig. 4) and a few previous publications showed that a larger proportion of the viral DNA in the brain tissues

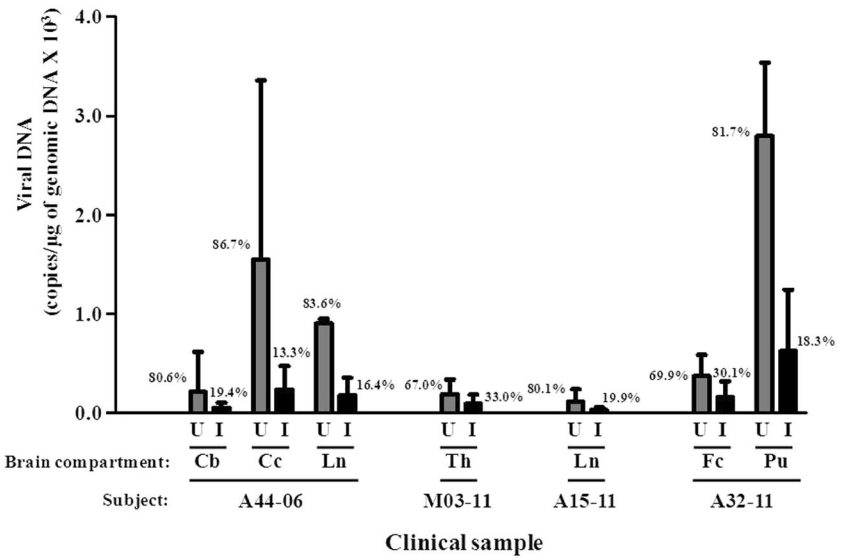


**Fig. 4** The relative proportion of the integrated viral DNA in different brain tissues. The absolute number of the total viral DNA copies from different neural and peripheral tissues was determined using a TaqMan probe-based real-time PCR targeting a 93-bp amplicon spanning the U5-PBS region. The absolute number of the integrated viral copies in the same genomic DNA samples was determined using a nested Alu-LTR PCR amplifying a 103 bp fragment spanning the R-U5 region. The data are representative of two independent experiments and presented as the mean of three to five replicate samples from each compartment±S.D. U and I represent the percent values of the unintegrated and integrated viral DNA copies, respectively, as shown. The subject and tissue identities are illustrated. *Cb* cerebellum, *Cc* cervical cord, *Fc* frontal cortex, *Ln* lymph node, *Th* thalamus, and *Pu* putamen

exists in the unintegrated form (Shaw et al. 1985; Pang et al. 1990; Teo et al. 1997).

We found that the overall DNA viral load across different brain compartments was low to moderate, typically in one to three digits per microgram of the genomic DNA (Table 3).

Importantly, we expressed the viral load in terms of copy number per microgram of genomic DNA rather than the weight of the brain tissue used for the DNA extraction, thus eliminating the variation in the recovery of the DNA from the tissues influencing the DNA copy number. Given that approximately 7.1 pg of genomic DNA constitute the genome of a normal human somatic cell, 1 μg of the genomic DNA is expected to have derived from $0.14\times10^6$ cells. Following this maxim, we found that the proviral load in our clinical samples to be low or moderate as reported by others previously. Bockstahler et al. reported a rate of one proviral DNA per 1000 cells in the brain tissue (Bockstahler et al. 1995). In our samples, we found one copy of the viral DNA per 432 cerebellar cells (324.3 copies/μg, subject A44-06, Table 3) or 6034 frontal cortex cells (23.2 copies/μg, subject A20-12, Table 3). Of note, although our analysis did not differentiate between the integrated and unintegrated forms of the virus, it reflected the overall viral DNA burden in the brain tissues. Of note, gene expression was reported from unintegrated viral DNA forms suggesting that these viral DNA forms can be of pathological significance (Stevenson et al. 1990; Wu 2004).

The low copy number proviral load distribution across the brain compartments is consistent with a few previous reports of subtype B infection (An et al. 1996; Fujimura et al. 1997).

Unlike a few earlier studies that reported an uneven viral distribution in the brain compartments, our study found a broadly uniform distribution of the viral DNA across different brain compartments and failed to see differential accumulation the viral DNA in any specific brain compartment. Importantly, there was no agreement among the previous publications, with respect to which brain compartment contains more viral burden. Achim et al. demonstrated higher levels of viral antigens and DNA in the deep gray matter (Achim et al. 1994). Fujimura et al. found larger proviral DNA load in the medial temporal lobe than in the frontal lobe (Fujimura et al. 1997). Brew et al. showed higher viral antigen expression in the globus pallidus than in the basal ganglia (Brew et al. 1995). Wiley et al. demonstrated higher levels of viral RNA in a few brain compartments such as the basal ganglia and hippocampus as compared to some others including the cerebellar cortex and mid-frontal cortical gray matter (Wiley et al. 1998). Examining eight different regions in the brain, Kumar et al. found that the viral transcript levels were significantly higher in the caudate nucleus (Kumar et al. 2007). To the best of our knowledge, unlike the previous studies, the present study is the first one to determine proviral DNA load in different brain compartments of subtype C infection. Additionally, unlike several previous studies, we used a highly sensitive real-time PCR technique to quantitate the viral DNA. As hypothesized previously, the proviral burden in the brain tissues in the early and late phases of the infection could be different (Bockstahler et al. 1995). The viral proliferation may be restricted to a few specific compartments in the early phases of the infection while in the late phases, the increased viral load may cause more uniform distribution across different brain tissues. It would be difficult to resolve this issue given that studies of this nature can be conducted only in the terminal stage using the brain tissues available following the death of the subjects.

To examine the phylogenetic relatedness between the viral sequences in brain and the peripheral tissues, we compared the V3–V5 envelope sequences within each subject. In three subjects (A1-13, A46-06, and M03-11), sequences only from the neural tissues were available hence such a comparison was not possible. In four of the cases (A15-11, MLC221-05, A46-06, and A26-10) a phylogenetic separation was evident, as expected, suggesting compartmentalized evolution of the viral sequences in the brain similar to that reported by others previously (Ohagen et al. 2003; Lamers et al. 2011). Interestingly, in the remaining three subjects (A32-11, A20-12, and M316-11), the V3–V5 sequences between the neural and non-neural tissues clustered together suggesting a lack of phylogenetic separation and a free exchange of the viruses between compartments possibly as a consequence of enhanced permeability between the brain and the blood in the advanced stages of the infection (Fig. 1). Future studies should attempt to confirm the phenomenon of free exchange of the viral strains between the brain and blood using lineage markers and single-cell sequencing techniques. For instance, CD163 is expressed only on perivascular macrophages, but not on microglial cells. And the significance of the $CD163^+CD16^+$ monocytes in blood has been implicated in the neuropathogenesis in rhesus macaques (Fischer-Smith et al. 2008). Our data in these three subjects are consistent with the proposition that viral dissemination is possible between the neural and non-neural compartments in the advanced stages of the viral infection (Alexaki et al. 2008). In a similar study, Burkala et al. compared envelope sequences derived from five subjects among three different compartments the spleen, brain and choroid plexus (Burkala et al. 2005). A clear separation between the brain- and spleen-derived sequences was evident only in three subjects. In two subjects (B and E), sequences from the three different compartments mixed freely suggesting dissemination of the viral sequences between blood and the brain. Likewise, Lamers et al. reported a significant phylogenetic overlap between the brain and peripheral compartments in their sequences especially in subjects who died of pathologies other than HIV-associated dementia (Lamers et al. 2011).

We acknowledge a major limitation of the current study. A possible contamination of the brain tissues with blood, in principle, could explain the phylogenetic relatedness between the env sequences of the neural and non-neural tissues in the

three subjects. Unfortunately, plasma samples were not available from the study subjects hence the genetic diversity of the env in the blood could not be determined and a comparison with the brain sequences could not be performed. We, however, believe that contamination was not a possible explanation underlying the observation. The possibility of viral DNA of the blood contaminating the brain tissue is insignificant given that the mean frequency of the blood cells containing an integrated virus is too small especially after washing the tissues to remove blood. As reviewed by Pace et al., the rate of the integrated viral copy numbers found in the peripheral blood, as estimated by many studies, was approximately only 1000 copies of DNA per million CD4 cells in regular progressors with the upper limit being 4.6 times higher (Pace et al. 2011). Although the CD4 counts of many of our study subjects is not known, considering the advanced stage of the infection in many of the subjects, the CD4 count and the impending integrated DNA burden is expected to be low. Furthermore, in four of the 10 subjects (A15-11, MLC221-05, A46-06, and A26-10), a phylogenetic separation of the env sequences between the neural and non-neural compartments was evident (Fig. 1) asserting against the possibility of contamination.

In our study, we determined a total of 54 envelope sequences derived from different neural and non-neural compartments of the 10 study subjects, spanning the V3 to V5 regions. A coreceptor use prediction of the V3 loop of the sequences using two different algorithms, the PSSM or the geno2pheno, indicated that all the sequences, with the exception of one subject, were R5-tropic (Table 2). In subject MLC221-05, env sequences derived from two different neural compartments, the frontal cortex, and the hippocampus, but not from others, predicted to be X4- or dual-tropic. The envelope sequences derived from frontal cortex and hippocampus of MLC221-05 demonstrated many unusual properties including the shorter V3 loop length (consisting of only 34 amino acids instead of 35), the deletion of the aspartic acid residue at position 25 of the V3 loop, the crown of the V3 loop containing the GPGK variation instead of the GPGQ motif typical of subtype C and the total positive charge of the V3 loop being unusually high for subtype C. All these molecular variations may have contributed to the unusual CXCR4 coreceptor preference of the two envelope sequences of the subject. Unlike in subtype B, the coreceptor switch from CCR5 to CXCR4 is highly uncommon in subtype C infections (Hartley et al. 2005). The significance of the presence of the envelope sequences that are X4- or dual-tropic in only two, but not other, brain compartments of MLC221-05 is not known. Phenotypic assays to characterize the coreceptor requirement of these envelopes will be necessary to confirm the bioinformatic predictions of our analyses. Thus, the predicted coreceptor preference of the env sequences was in line with the expected preference of subtype C and of the brain-derived sequences (Gorry et al. 2001; Ohagen et al. 2003).

Of note, a striking difference was found in the length of the V4 loop in all the ten subjects examined, regardless of the tissue origin. The V4 loop was subjected to extensive deletion in all the subjects, the significance of which is not clear (Fig. 2). While the length of the V4 loop in HXB2 and Indie-C1 consists of 34 and 32 amino acids, respectively, the loop consisted of 21–35 amino acid residues in the sequences examined. A previous analysis demonstrated that while in subtype B, the V4 loop length ranges between 26 and 40 residues, in subtype C, the loop tends to be shorter ranging between 20 and 37 residues (Gnanakaran et al. 2007). Thus, a shorter V4 loop appears to be characteristic of subtype C. Shorter V1/V2 loop of env are proposed to be associated with enhanced affinity for receptors (Chohan et al. 2005). The biological significance of shorter V4 loop in subtype C remains to be evaluated.

In summary, the present analysis of viral env sequences derived from several neural and non-neural tissues of 10 HIV-1 seropositive subjects, in advanced stages of the infection, demonstrated uniform distribution of the proviral burden among the brain compartments without a preferential accumulation of the viral DNA in any specific compartment. A large majority of the envelope sequences demonstrated CCR5-tropism as expected. In a subset of the subjects, a free exchange of the viral sequences between the neural and peripheral compartments was identified. A simultaneous determination of the presence of the viral antigens, the viral transcripts, and the proviral DNA in different brain compartments may shed more light on the significance of the viral burden to neurologic consequences in the viral infection.

## Methods

### The clinical samples

The tissue samples, neural and non-neural, were collected from HIV-1 infected subjects within 20 h after death following postmortem, between 2005 and 2013 and stored at the Human Brain Tissue Repository, NIMHANS, Bangalore, India. The sample collection was performed after obtaining an informed consent from close relatives and with the approval of the Institutional Scientific Ethics Committee, NIMHANS. The tissues derived from nine different neural (frontal cortex, hippocampus, caudate, putamen, thalamus, amygdala, cerebellum, cervical cord and choroid plexus) and three peripheral (liver, paratracheal lymph node, and spleen) compartments were snap frozen and then stored in the deep freezer at −80 °C until use. Tissue samples were transported to JNCASR on dry-ice for the molecular biology work. The clinical profile of the ten study subjects is summarized (Table 1).

Of the ten subjects, who were all drug-naive, seven were afflicted with opportunistic infections of the brain such as toxoplasmosis, TBM, GB syndrome, disseminated tuberculosis and cryptococcal meningitis, and associated GB syndrome. These subjects therefore belong to CDC Stage C (as per CDC staging, even in the absence of CD4 counts) or Clinical Stage 4 as per the WHO clinical staging system.

Tissue samples (20–50 mg) deposited in a fresh 1.5 ml plastic vial were homogenized using a micropestle (Z317314-1PAK, Sigma Aldrich, St Louis, MO, USA). Prior to homogenization, we took the precaution to wash the minced brain tissues multiple times to remove blood cells that may harbor the viral DNA of the peripheral compartment. The samples were subjected to 15–20 pulses until a clear homogenate was formed. Genomic DNA was extracted from the homogenized samples using a commercial kit (GeneElute mammalian genomic DNA mini-prep kit, Sigma Aldrich, St Louis, MO, USA) as per the manufacturer's instructions. The DNA concentration in the extracted samples was quantitated using a spectrophotometer (ND-1000 spectrophotometer, NanoDrop Technologies, Wilmington, USA) and 250 ng of the DNA was used for the envelope amplification. A nested-PCR approach was used to amplify a 700-bp fragment consisting of the V3–V5 region in the envelope using the heteroduplex mobility assay kit (The NIH AIDS Research and Reference program). Primers ED5 (forward- 5′-ATGGGATCAAAGCC TAAAGCCATGTG-3′) and ED12 (reverse- 5′-AGTGCT TCCTGCTGCTCCCAAGAACCCAAG-3′) were used in the first round of the amplification and primers ES7 (F-5′ TGTAAAACGACGGCCAGTCTGTTAAATGGC AGTCTAGC 3′) and ES8 (R-5′ CAGGAAACAGCTAT GACCCACTTCTCCAATTGTCCCTCA 3′) in the second round. The PCR reaction conditions were the same for both the rounds of amplification. The samples were denatured at 91 °C for 15 s, annealed at 55 °C for 45 s and extended at 72 °C for 1 min followed by a final extension for 5 min. The first-round amplification was performed for 35 cycles and 2 μl of the amplified product were transferred to the second round. The amplification reaction of 25 μl contained 100 nM of each primer, 100 μM of each dNTP and 0.25 unit of Taq-DNA polymerase, XT-20 PCR system (Genei, Redmond, Washington, USA). The PCR fragment was purified using a commercial kit (DNA Gel-PCR purification mini-prep kit, Xcelris genomics, Ahmedabad, India) and sequenced using the M13 sequencing primer (5′-GTAAAACGACGGCCAGT-3′). DNA sequencing was performed on the ABI 377 automated sequencer using the ABI PRISM™ Dye Terminator Cycle Sequencing Ready Reaction Kit. Every individual gene sequence was subjected to the BLAST analysis against the laboratory sequence database to confirm authenticity. The envelope sequences reported here are available under the accession numbers KM513799–KM513852 from Genbank.

### Phylogenetic analysis and subtype identification

As a standard quality control measure, all the sequences were blasted against the Los Alamos HIV sequence database (http://www.hiv.lanl.gov) as well as the laboratory database to rule out the possibility of laboratory-generated contamination. HIV-1 reference sequences were downloaded from the Los Alamos database (http://www.hiv.lanl.gov/components/sequence/HIV/search/search.html). The sequences were aligned using Bioedit Sequence Alignment Editor-ClustalW Multiple alignment and the gaps were manually edited to keep equal number of nucleotides for each sequence. The molecular evolutionary genetic analysis (MEGA5) software was used to construct the neighbor-joining (NJ) tree with a selected model and 1000 bootstrap replications. The nodal bootstrap values selected for the tree were ≥70 %. After obtaining the NJ tree, the tree was edited to display in the best fit mode. The reference subtype B (HXB2, K03455) and subtype C (Indie-C1, AB023804), envelope sequences were used in the multiple sequence alignment. The potential *N*-glycosylation sites were identified using the software http://www.cbs.dtu.dk/services/NetNGlyc/. The subtype identity of each sequence was determined using the genotyping tool http://www.ncbi.nlm.nih.gov/projects/genotyping/genotype.cgi located at NCBI.

### Prediction of the coreceptor preference of V3

Coreceptor tropism of the V3 loop sequences was predicted using the position-specific scored matrix "PSSM" available at http://fortinbras.us/cgi-bin/fssm/fssm.pl. Higher and lower PSSM scores are suggestive of the CXCR4 and CCR5 use, respectively. The amino acid sequences of third variable region of all the envelope sequences obtained from the tissue sample were used to generate a matrix of likelihood ratio scores for each site in the sequences. Additionally, the charge profile of the V3 loop (the 11/25 rule) was also evaluated using geno2pheno available at http://indra.mullins.microbiol.washington.edu/webpssm/. The false positive rate percentage (FPR%) in geno2pheno analysis was calculated taking the cut off value as 10 %. Net charge of V3 has been calculated through http://indra.mullins.microbiol.washington.edu/webpssm.

### Measurement of proviral DNA load in the tissue samples

A TaqMan probe-based real-time PCR was developed to determine the HIV-1 proviral DNA load in the genomic DNA samples extracted from different neural and peripheral tissue samples. A 93-bp region spanning the U5-PBS region of the LTR, highly conserved among all the HIV-1 subtypes, was

selected for the amplification. The forward primer N2185 (5′-TAGTGTGTGCCCGTCTGTTG-3′, HXB2 554–573) and the reverse primer N2186 (5′-TTCGGGCGCCACTGCTAGA-3′, reverse complement, HxB2 628–646) were used in the amplification in combination with the TaqMan probe N2187 (5′-ACTCTGGTAACTAGAGATCCCTCAGACC-3′, HxB2 578–605) that was labeled with 6-carboxyfluorescein (FAM) at the 5′ end and 6-carboxytetramethyl rhodamine (TAMRA) at the 3′ end. For the purpose of normalization, the house-keeping gene glyceraldehydes-3-phosphate dehydrogenase (GAPDH) was used. The forward primer N2211 (5′-GTGAACCATGAGAAGTATGACAAC-3′) and the reverse primer N2212 (5′-CATGAGTCCTTCCACGATACC-3′) were used in combination with the TaqMan probe, N2213 (5′-CCTCAAGATCATCAGCAATGCCTCCTG-3′) that was labeled with FAM and TAMRA at the 5′ and 3′ ends, respectively. The amplification reaction mixture of 25 μl volume contained 200 μM of each dNTP, 50 mM $MgCl_2$, 100 nM of each of the primers, 200 nM of Taqman probe, 0.5 unit of MyTaq™ HS DNA polymerase (Bioline reagents limited, London, UK), and 500 ng of genomic DNA. The amplification conditions consisted of an initial denaturation step of 3 min at 95 °C followed by thermal cycling for 40 cycles of denaturation at 91 °C for 15 s and annealing and extension for 1 min at 60 °C. The amplification was performed using a real-time PCR machine (CFX96™ Real-Time System, BioRad).

A standard curve was generated with each of the amplifications using genomic DNA extracted from HLM-1 cells that contain a single copy of the integrated provirus per cell. The standard curve was constructed using known number of proviral copy number spanning from 10 to 10,000 copies per reaction. Each amplification reaction, including that of the standard curves, consisted of triplicate wells. Total amount of DNA added to each reaction was kept constant using genomic DNA extracted from HeLa cells that were not infected. The GAPDH PCR consisting of a fixed quantity of the genomic DNA accompanied the HIV-1 PCR and the threshold cycle ($C_t$) values of the former were used to normalize the latter. The HIV PCR values were not considered if the GAPDH PCR values differed by more than 0.5 $C_t$ numbers. The HIV-1 proviral copy number was derived from the regression analysis of the HLM-1 standard curve using the formula $[\text{Product}_T=(\text{Template}_i)2^n]$ where $n$ is the number of cycle, i is the "initial template number".

To circumvent the problem of uneven distribution of the virus-infected pockets within the tissues of a brain compartment, we collected multiple samples from different zones of each tissue (five or six) and processed them independently and simultaneously through DNA extraction and real-time PCR. The quantitation was repeated at least one more time and mostly two times. The viral load was determined as the arithmetic mean of all the positive results for a tissue compartment of each subject. Standard quality control measures were implemented stringently to avoid contamination. Each assay contained multiple vials that lacked template DNA or contained genomic DNA extracted from control brain tissues. In each independent DNA extraction, brain tissues of two seronegative controls were included to ensure the authenticity of the amplification. The proviral load was expressed as copy number detected per microgram of genomic DNA thus normalizing for the differences in the DNA extraction from the tissues. At the time of assay optimization, to ensure efficient recovery of the genomic DNA from the tissue samples, known amount of genomic DNA was added to uninfected brain tissue samples prior to homogenization. Following homogenization of the tissues and DNA extraction, the real-time PCRs were performed to quantitate the amount of the pulsed proviral DNA recovered. The recovery of the genomic DNA was found highly efficient typically around 90–95 % of the pulsed DNA. The HIV PCR was highly efficient and sensitive consistently detecting less than 10 copies of the viral template. The standard curve reproducibly generated a high level of coefficient value ($R^2>0.99$).

Quantification of integrated DNA using a nested Alu-PCR. The first round of the nested Alu-LTR PCR was performed using the forward primer N2208 (5′-GATCTGAGCCTGGGAGCTCTCTG-3′ HXB2 474–491) located in R region and a reverse primer N1740 (5′-TGCTGGGATTACAGGCGTGAG-3′) located in the Alu-repeats of cellular genomic DNA. A mixed population of the PCR products was amplified in the first round of the PCR. The second-round of the PCR was performed using an inner set of primers N2481 (5′-AACTAGGGAACCCACTGCTTAAG-3′, HXB2 500–523) and N2209 (5′-TCTGAGGGATCTCTAGTTACCAGAGTC-3′, HXB2 577–603) that amplifies a 103-bp fragment spanning the R-U5 region. To generate a standard curve for measuring the integrated viral copy number, Jurkat cells infected with a VSV-G pseudotyped GFP reporter virus containing Indie-C1 LTR at a high M.O.I. of 0.4 and selected over a period of 3 weeks to ensure representation of diverse integration events were used. At the end of the selection period, the infected cell pool contained an integration incidence of 3.7± 0.64 copies per cell as quantified using a real-time PCR with primers N2208 and N2209. The genomic DNA extracted from these cells was used to generate an integration DNA standard curve ranging from 1 to $10^5$ copies/cell. The number of the unknown viral integration events in the samples was quantified by regression analysis using the standard curve.

**Acknowledgments** This study was supported by grants from the Department of Science and Technology, India under the Indo-Brazil Research program (DST/INT/Brazil/RPO-02/2009(i)) and intramural grants from JNCASR to UR. MM was supported by a post-doctoral fellowship and SD by a student fellowship from JNCASR. AV is a recipient of the

Council of Science and Industrial Research fellowship from the Government of India.

**Conflict of interest** The authors state that they have no conflict of interest.

## References


Achim CL, Wang R, Miners DK, Wiley CA (1994) Brain viral burden in HIV infection. J Neuropathol Exp Neurol 53:284–294

Albini A, Benelli R, Giunciuglio D, Cai T, Mariani G, Ferrini S, Noonan DM (1998) Identification of a novel domain of HIV tat involved in monocyte chemotaxis. J Biol Chem 273:15895–15900

Alexaki A, Liu Y, Wigdahl B (2008) Cellular reservoirs of HIV-1 and their role in viral persistence. Curr HIV Res 6:388–400

An SF, Giometto B, Scaravilli F (1996) HIV-1 DNA in brains in AIDS and pre-AIDS: correlation with the stage of disease. Ann Neurol 40: 611–617

An SF, Groves M, Gray F, Scaravilli F (1999) Early entry and widespread cellular involvement of HIV-1 DNA in brains of HIV-1 positive asymptomatic individuals. J Neuropathol Exp Neurol 58:1156–1162

Antinori A, Arendt G, Becker JT, Brew BJ, Byrd DA, Cherner M, Clifford DB, Cinque P, Epstein LG, Goodkin K, Gisslen M, Grant I, Heaton RK, Joseph J, Marder K, Marra CM, McArthur JC, Nunn M, Price RW, Pulliam L, Robertson KR, Sacktor N, Valcour V, Wojna VE (2007) Updated research nosology for HIV-associated neurocognitive disorders. Neurology 69:1789–1799

Bachu M, Yalla S, Asokan M, Verma A, Neogi U, Sharma S, Murali RV, Mukthey AB, Bhatt R, Chatterjee S, Rajan RE, Cheedarla N, Yadavalli VS, Mahadevan A, Shankar SK, Rajagopalan N, Shet A, Saravanan S, Balakrishnan P, Solomon S, Vajpayee M, Satish KS, Kundu TK, Jeang KT, Ranga U (2012) Multiple NF-kappaB sites in HIV-1 subtype C long terminal repeat confer superior magnitude of transcription and thereby the enhanced viral predominance. J Biol Chem 287:44714–44735

Bell JE, Busuttil A, Ironside JW, Rebus S, Donaldson YK, Simmonds P, Peutherer JF (1993) Human immunodeficiency virus and the brain: investigation of virus load and neuropathologic changes in pre-AIDS subjects. J Infect Dis 168:818–824

Bockstahler LE, Werner T, Festl H, Weis S, Einhaeup KM, Erfle V, Brack-Werner R (1995) Distribution of HIV genomic DNA in brains of AIDS patients. Clin Diagn Virol 3:61–72

Brew BJ, Rosenblum M, Cronin K, Price RW (1995) AIDS dementia complex and HIV-1 brain infection: clinical-virological correlations. Ann Neurol 38:563–570

Briggs DR, Tuttle DL, Sleasman JW, Goodenow MM (2000) Envelope V3 amino acid sequence predicts HIV-1 phenotype (co-receptor usage and tropism for macrophages). AIDS 14:2937–2939

Burkala EJ, He J, West JT, Wood C, Petito CK (2005) Compartmentalization of HIV-1 in the central nervous system: role of the choroid plexus. AIDS 19:675–684

Chan LG, Kandiah N, Chua A (2012) HIV-associated neurocognitive disorders (HAND) in a South Asian population—contextual application of the 2007 criteria. BMJ Open 2:e000662

Chohan B, Lang D, Sagar M, Korber B, Lavreys L, Richardson B, Overbaugh J (2005) Selection for human immunodeficiency virus type 1 envelope glycosylation variants with shorter V1-V2 loop sequences occurs during transmission of certain genetic subtypes and may impact viral RNA levels. J Virol 79:6528–6531

Cilliers T, Nhlapo J, Coetzer M, Orlovic D, Ketas T, Olson WC, Moore JP, Trkola A, Morris L (2003) The CCR5 and CXCR4 coreceptors are both used by human immunodeficiency virus type 1 primary isolates from subtype C. J Virol 77:4449–4456

Esparza J, Bhamarapravati N (2000) Accelerating the development and future availability of HIV-1 vaccines: why, when, where, and how? Lancet 355:2061–2066

Fischer-Smith T, Croul S, Sverstiuk AE, Capini C, L'Heureux D, Regulier EG, Richardson MW, Amini S, Morgello S, Khalili K, Rappaport J (2001) CNS invasion by CD14+/CD16+ peripheral blood-derived monocytes in HIV dementia: perivascular accumulation and reservoir of HIV infection. J Neurovirol 7:528–541

Fischer-Smith T, Bell C, Croul S, Lewis M, Rappaport J (2008) Monocyte/macrophage trafficking in acquired immunodeficiency syndrome encephalitis: lessons from human and nonhuman primate studies. J Neurovirol 14:318–326

Fujimura RK, Goodkin K, Petito CK, Douyon R, Feaster DJ, Concha M, Shapshak P (1997) HIV-1 proviral DNA load across neuroanatomic regions of individuals with evidence for HIV-1-associated dementia. J Acquir Immune Defic Syndr Hum Retrovirol 16:146–152

Gartner S, Liu Y (2002) Insights into the role of immune activation in HIV neuropathogenesis. J Neurovirol 8:69–75

Glass JD, Wesselingh SL, Selnes OA, McArthur JC (1993) Clinical-neuropathologic correlation in HIV-associated dementia. Neurology 43:2230–2237

Glass JD, Fedor H, Wesselingh SL, McArthur JC (1995) Immunocytochemical quantitation of human immunodeficiency virus in the brain: correlations with dementia. Ann Neurol 38:755–762

Gnanakaran S, Lang D, Daniels M, Bhattacharya T, Derdeyn CA, Korber B (2007) Clade-specific differences between human immunodeficiency virus type 1 clades B and C: diversity and correlations in C3-V4 regions of gp120. J Virol 81:4886–4891

Gonzalez RG, Cheng LL, Westmoreland SV, Sakaie KE, Becerra LR, Lee PL, Masliah E, Lackner AA (2000) Early brain injury in the SIV-macaque model of AIDS. AIDS 14:2841–2849

Gonzalez-Scarano F, Martin-Garcia J (2005) The neuropathogenesis of AIDS. Nat Rev Immunol 5:69–81

Gorry PR, Bristol G, Zack JA, Ritola K, Swanstrom R, Birch CJ, Bell JE, Bannert N, Crawford K, Wang H, Schols D, De CE, Kunstman K, Wolinsky SM, Gabuzda D (2001) Macrophage tropism of human immunodeficiency virus type 1 isolates from brain and lymphoid tissues predicts neurotropism independent of coreceptor specificity. J Virol 75:10073–10089

Gupta JD, Satishchandra P, Gopukumar K, Wilkie F, Waldrop-Valverde D, Ellis R, Ownby R, Subbakrishna DK, Desai A, Kamat A, Ravi V, Rao BS, Satish KS, Kumar M (2007) Neuropsychological deficits in human immunodeficiency virus type 1 clade C-seropositive adults from South India. J Neurovirol 13:195–202

Hartley O, Klasse PJ, Sattentau QJ, Moore JP (2005) V3: HIV's switch-hitter. AIDS Res Hum Retrovir 21:171–189

Heaton RK, Grant I, Butters N, White DA, Kirson D, Atkinson JH, McCutchan JA, Taylor MJ, Kelly MD, Ellis RJ (1995) The HNRC 500—neuropsychology of HIV infection at different disease stages. HIV Neurobehavioral Research Center. J Int Neuropsychol Soc 1: 231–251

Jensen MA, Li FS, 't Wout AB, Nickle DC, Shriner D, He HX, McLaughlin S, Shankarappa R, Margolick JB, Mullins JI (2003) Improved coreceptor usage prediction and genotypic monitoring of R5-to-X4 transition by motif analysis of human immunodeficiency virus type 1 env V3 loop sequences. J Virol 77:13376–13388

Jensen MA, Coetzer M, 't Wout AB, Morris L, Mullins JI (2006) A reliable phenotype predictor for human immunodeficiency virus type 1 subtype C based on envelope v3 sequences. J Virol 80: 4698–4704

Johnson RT, Glass JD, McArthur JC, Chesebro BW (1996) Quantitation of human immunodeficiency virus in brains of demented and nondemented patients with acquired immunodeficiency syndrome. Ann Neurol 39:392–395

Kumar AM, Borodowsky I, Fernandez B, Gonzalez L, Kumar M (2007) Human immunodeficiency virus type 1 RNA Levels in different

regions of human brain: quantification using real-time reverse transcriptase-polymerase chain reaction. J Neurovirol 13:210–224

Lamers SL, Gray RR, Salemi M, Huysentruyt LC, McGrath MS (2011) HIV-1 phylogenetic analysis shows HIV-1 transits through the meninges to brain and peripheral tissues. Infect Genet Evol 11:31–37

Lazarini F, Seilhean D, Rosenblum O, Suarez S, Conquy L, Uchihara T, Sazdovitch V, Mokhtari K, Maisonobe T, Boussin F, Katlama C, Bricaire F, Duyckaerts C, Hauw JJ (1997) Human immunodeficiency virus type 1 DNA and RNA load in brains of demented and nondemented patients with acquired immunodeficiency syndrome. J Neurovirol 3:299–303

Liu Y, Tang XP, McArthur JC, Scott J, Gartner S (2000) Analysis of human immunodeficiency virus type 1 gp160 sequences from a patient with HIV dementia: evidence for monocyte trafficking into brain. J Neurovirol 6(Suppl 1):S70–S81

Mahadevan A, Shankar SK, Satishchandra P, Ranga U, Chickabssaviah YT, Vani S, Ravi V, Pardo CA, Nath A, Zinc MC (2007) Characterization of human immunodeficiency virus (HIV)-infected cells in infiltrates associated with CNS opportunistic infections in patients with HIV clade C infection. J Neuropathol Exp Neurol 66: 799–808

Muniyandi K, Venkatesan J, Arutselvi T, Jayaseelan V (2012) Study to assess the prevalence, nature and extent of cognitive impairment in people living with AIDS. Indian J Psychiatry 54:149–153

Novitsky V, Woldegabriel E, Kebaabetswe L, Rossenkhan R, Mlotshwa B, Bonney C, Finucane M, Musonda R, Moyo S, Wester C, van Widenfelt E, Makhema J, Lagakos S, Essex M (2009) Viral load and CD4+ T-cell dynamics in primary HIV-1 subtype C infection. J Acquir Immune Defic Syndr 50:65–76

Ohagen A, Devitt A, Kunstman KJ, Gorry PR, Rose PP, Korber B, Taylor J, Levy R, Murphy RL, Wolinsky SM, Gabuzda D (2003) Genetic and functional analysis of full-length human immunodeficiency virus type 1 env genes derived from brain and blood of patients with AIDS. J Virol 77:12336–12345

Pace MJ, Agosto L, Graf EH, O'Doherty U (2011) HIV reservoirs and latency models. Virology 411(2):344–54

Pang S, Koyanagi Y, Miles S, Wiley C, Vinters HV, Chen IS (1990) High levels of unintegrated HIV-1 DNA in brain tissue of AIDS dementia patients. Nature 343:85–89

Persidsky Y, Zheng J, Miller D, Gendelman HE (2000) Mononuclear phagocytes mediate blood–brain barrier compromise and neuronal injury during HIV-1-associated dementia. J Leukoc Biol 68:413–422

Pollakis G, Kang S, Kliphuis A, Chalaby MI, Goudsmit J, Paxton WA (2001) N-linked glycosylation of the HIV type-1 gp120 envelope glycoprotein as a major determinant of CCR5 and CXCR4 coreceptor utilization. J Biol Chem 276:13433–13441

Ranga U, Shankarappa R, Siddappa NB, Ramakrishna L, Nagendran R, Mahalingam M, Mahadevan A, Jayasuryan N, Satishchandra P, Shankar SK, Prasad VR (2004) Tat protein of human immunodeficiency virus type 1 subtype C strains is a defective chemokine. J Virol 78:2586–2590

Rao VR, Sas AR, Eugenin EA, Siddappa NB, Bimonte-Nelson H, Berman JW, Ranga U, Tyor WR, Prasad VR (2008) HIV-1 clade-specific differences in the induction of neuropathogenesis. J Neurosci 28:10010–10016

Riedel D, Ghate M, Nene M, Paranjape R, Mehendale S, Bollinger R, Sacktor N, McArthur J, Nath A (2006) Screening for human immunodeficiency virus (HIV) dementia in an HIV clade C-infected population in India. J Neurovirol 12:34–38

Sacktor N, McDermott MP, Marder K, Schifitto G, Selnes OA, McArthur JC, Stern Y, Albert S, Palumbo D, Kieburtz K, De Marcaida JA, Cohen B, Epstein L (2002) HIV-associated cognitive impairment before and after the advent of combination therapy. J Neurovirol 8: 136–142

Saini S, Barar KV (2014) Assessment of neurocognitive functions in HIV/AIDS patients on HAART using the international HIV dementia scale. Int J Nutr Pharmacol Neurol Dis 4:252–255

Satishchandra P, Nalini A, Gourie-Devi M, Khanna N, Santosh V, Ravi V, Desai A, Chandramuki A, Jayakumar PN, Shankar SK (2000) Profile of neurologic disorders associated with HIV/AIDS from Bangalore, south India (1989–96). Indian J Med Res 111:14–23

Shankar SK, Mahadevan A, Satishchandra P, Kumar RU, Yasha TC, Santosh V, Chandramuki A, Ravi V, Nath A (2005) Neuropathology of HIV/AIDS with an overview of the Indian scene. Indian J Med Res 121:468–488

Shaw GM, Harper ME, Hahn BH, Epstein LG, Gajdusek DC, Price RW, Navia BA, Petito CK, O'Hara CJ, Groopman JE (1985) HTLV-III infection in brains of children and adults with AIDS encephalopathy. Science 227:177–182

Siddappa NB, Dash PK, Mahadevan A, Desai A, Jayasuryan N, Ravi V, Satishchandra P, Shankar SK, Ranga U (2005) Identification of unique B/C recombinant strains of HIV-1 in the southern state of Karnataka, India. AIDS 19:1426–1429

Singh R, Kaur M, Arora D (2011) Neurological complications in late-stage hospitalized patients with HIV disease. Ann Indian Acad Neurol 14:172–177

Stevenson M, Haggerty S, Lamonica CA, Meier CM, Welch SK, Wasiak AJ (1990) Integration is not necessary for expression of human immunodeficiency virus type 1 protein products. J Virol 64:2421–2425

Teo I, Veryard C, Barnes H, An SF, Jones M, Lantos PL, Luthert P, Shaunak S (1997) Circular forms of unintegrated human immunodeficiency virus type 1 DNA and high levels of viral protein expression: association with dementia and multinucleated giant cells in the brains of patients with AIDS. J Virol 71:2928–2933

Wadia RS, Pujari SN, Kothari S, Udhar M, Kulkarni S, Bhagat S, Nanivadekar A (2001) Neurological manifestations of HIV disease. J Assoc Physicians India 49:343–348

White DA, Heaton RK, Monsch AU (1995) Neuropsychological studies of asymptomatic human immunodeficiency virus-type-1 infected individuals. The HNRC Group. HIV Neurobehavioral Research Center. J Int Neuropsychol Soc 1:304–315

Wiley CA, Masliah E, Achim CL (1994) Measurement of CNS HIV burden and its association with neurologic damage. Adv Neuroimmunol 4:319–325

Wiley CA, Soontornniyomkij V, Radhakrishnan L, Masliah E, Mellors J, Hermann SA, Dailey P, Achim CL (1998) Distribution of brain HIV load in AIDS. Brain Pathol 8:277–284

Wu Y (2004) HIV-1 gene expression: lessons from provirus and non-integrated DNA. Retrovirology 1:13

Zhang H, Tully DC, Zhang T, Moriyama H, Thompson J, Wood C (2010) Molecular determinants of HIV-1 subtype C coreceptor transition from R5 to R5X4. Virology 407(1):68–79

Zhou L, Saksena NK (2013) HIV associated neurocognitive disorders. Infect Dis Rep 5:e8

Zink MC, Suryanarayana K, Mankowski JL, Shen A, Piatak MJ, Spelman JP, Carter DL, Adams RJ, Lifson JD, Clements JE (1999) High viral load in the cerebrospinal fluid and brain correlates with severity of simian immunodeficiency virus encephalitis. J Virol 73: 10480–10488